Available online www.jocpr.com

Journal of Chemical and Pharmaceutical Research, 2016, 8(10):196-203

Research Article

ISSN : 0975-7384
CODEN(USA) : JCPRC5

A Highly Active Catalyst Rh/5A for Preferential CO Oxidation in H_2- Rich Gas

Fang Wang

Department of Chemical Engineering, Binzhou University, China

---

ABSTRACT

A series of 5A-zeolite supported Rh catalysts were prepared using conventional impregnation method and their catalytic performances for CO preferential oxidation (PROX) in the presence of H_2-rich steam were investigate extensively. The effects of calcination temperature, Rh loading amount and the existence of moisture have been studied in detail. 1.2Rh/5A catalyst calcined at 400 ^oC showed an attractive catalytic performance, CO can be completely converted at 110^oC with a high selectivity of 70%. The structural characters of the Rh/5A catalysts were characterized by X-ray diffraction (XRD), X-ray photoelectron spectroscopy (XPS), and transmission electron Microscopy (TEM). The characterization results show that the high dispersion of Rh particles and reasonable pore size of 5A-zelite can be responsible for the attractive performance.

Keywords: 5A-zeolite; Rh; CO oxidation; PROX

INTRODUCTION

Hydrogen, as a source of energy for stationary power plants and moving vehicles, will certainly be widely used in a decade or so and is now in trials in several cities world-wide. The polymer electrolyte fuel cell (PEFC) can generate electricity without polluting the environment. Hydrogen is finally used as a fuel in this system. It is known that hydrogen can be supplied by various methods, for example, steam reforming of methanol, gasoline, and so on. When hydrogen is produced via the reforming reaction, the gas always contains CO as a poisoning impurity. Therefore, the hydrogen production system must be equipped with a CO removal system. Selective oxidation of CO in H_2-rich gas is one of the methods for lowering the CO concentration, Ideally, the catalyst must selectively oxidize up to about 1% (10,000 ppm) CO to less than 5 ppm while oxidizing as little of the H_2 as possible.

Supported Au [1], Ag [2], Cu [3], Pt group [4, 5], and metal oxides catalysts [6] have been developed for the selective CO oxidation in H_2-rich gas. However, the most investigated catalysts for surface reconstruction during adsorption and reaction processes are Rh catalysts [7-11]. Many investigations have been carried out in order to improve the knowledge about the influence of the catalyst nature on the catalytic behavior. Kimio et al [12] have found that K_2CO_3-promoted Rh/SiO_2 and Rh/USY catalysts exhibited much higher performance for selective CO oxidation in H_2-rich stream than Rh/SiO_2 and Rh/USY catalysts. Chuang et al [13] were the first to observe that adsorption of CO over Rh^0 crystallite on SiO_2 or Al_2O_3 caused disruption of the Rh^0 crystallites.

Since zeolites are attractive also because of their low cost and high thermal stability, recent studies had indicated that the use of zeolites as supports for platinum catalysts was promising to improve the catalyst selectivity, probably owing to the molecular sieve effects [14-16]. In particular, Pt-A catalysts resulted in the most selective among those tested (Pt-mordenite, Pt-X, Pt-A and Pt-Al_2O_3) [17].

In this paper, the catalytic activities of 5A zeolites-supported Rh catalyst for preferential CO oxidation were investigated. Particular attentions were paid to the catalytic activity, selectivity in H_2, H_2O rich stream as a function

of temperature and catalyst stability, the effect of Rh loading and calcinations temperature. The structural characters of the Rh/5A catalysts were comparatively investigated by TEM, XRD, and XPS measurements.

EXPERIMENTAL SECTION

Preparation

A series of catalysts used in this study were prepared by incipient wetness impregnation method, 5A zeolite was used as a support material; it was calcined at 650 ^{0}C for 5 h under atmosphere. Rh/5A catalysts were prepared by impregnation of 5A zeolites powder support with an aqueous solution of $RhCl_3.3H_2O$ and the mixture was stirred for 2h at about 60 ◦C. The samples were irradiated under infrared lamp and then dried at 110 ^{0}C overnight, followed by calcined at 200, 300, 400, and 500 ◦C in the air for 3h, respectively. Prior to the measurement, the catalysts were reduced at 300 ◦C in the stream of hydrogen with the flow rate of 30 ml min^{-1} for 1 h, and then cooled in hydrogen atmosphere to a room temperature.

Characterization of catalysts

Powder X-ray diffraction (XRD) analysis was performed to verify the species present in the catalysts. XRD patterns of the samples were recorded on a Rigaku D/MAX–RB X-ray diffractometer (with a target of Cu Kα) operated at 50 kV and 40 mA with a scanning rate of 0.5°/min and a scanning angle (2 theta) range of 10–90 °. Transmission electron microscopy (TEM) experiments were carried out to study the fine structure and morphology of the Au species dispersed in catalysts, using a JEOL TEM-1200EX Microscope operated at 120 kV. The samples were dispersed in ethanol by sonication and dropped on a copper grid coated with a carbon film. Chemical states of the atoms in the catalyst surface were investigated by X-ray photoelectron spectroscopy (XPS) on a VG ESCALAB 210 Electron Spectrometer (Mg Ka radiation; hν = 1253.6 eV). XPS data were calibrated using the binding energy of C1s (284.6 eV) as the standard.

Activity measurements

Catalytic performances tests were carried out in a fixed bed continuous flow quartz reactor (i.d.5 mm) at normal pressure and temperature from 70 to 180 ^{0}C. Typically, 200 mg of the catalyst was used in each run. All catalysts were reduced in situ by 50% H_2 in N_2 stream (flow rate 60 ml/min) at 300 ^{0}C for 1 h prior to use. The total flow rate of the feed gas was 75 ml/min (GHSV =22,500 h^{-1}). The feed gas consisted of 70 % of H_2, 2.0 % of CO and 1.4 % of O_2 in N_2 balance. Argon was used as a carrier gas and Nitrogen was used as internal standard for gas analysis. The gas phase effluents were analyzed on two on-line chromatographs equipped with thermal-conductivity detectors (TCD). At the end of the catalytic tests, the catalyst was cooled under N_2 stream and stored for characterizations in N_2 atmosphere. The catalytic activities were defined in terms of conversions of CO, conversion of O_2 and selectivities to CO_2. Conversions of CO was denoted as *CO%*, conversion of O_2 was denote as O_2*%* and selectivities to CO_2 was denoted as *S* which were calculated according to the corresponding equations:.

$$CO\ \% = \{([CO]_{in} - [CO]_{out})/ [CO]_{in}\} \times 100$$

$$O_2\ \% = \{([O_2]_{in} - [O_2]_{out})/ [O_2]_{in}\} \times 100$$

$$S\ \% = \{0.5 \times [CO_2]/ ([CO]_{in} - [CO]_{out})\} \times 100$$

RESULTS AND DISCUSSION

Catalyst characterization

XRD:

X-ray diffraction was used to estimate the mean rhodium particle size in the catalysts calcined at different temperatures and the results are shown in Figure 1 It can be found that the framework of 5A-zeolite was appeared in all of the samples. There was no detectable crystallite formation of the Rh spices over the catalysts calcined at 200 (a), which indicated that Rh species are highly dispersed in the 5A zeolites supports. For the catalyst calcined at 400°C (c), however, a border diffraction peak of Rh appear at 2θ= 41.0 ^{0}, corresponding to the Rh (1 1 1) faces. When the calcination temperature increased to 500°C (c), the diffraction peak of Rh became narrower and sharper, compared with catalyst (a, b), which indicated that the diameter of metal particles becomes larger according to polycrystal X-ray diffraction theory.

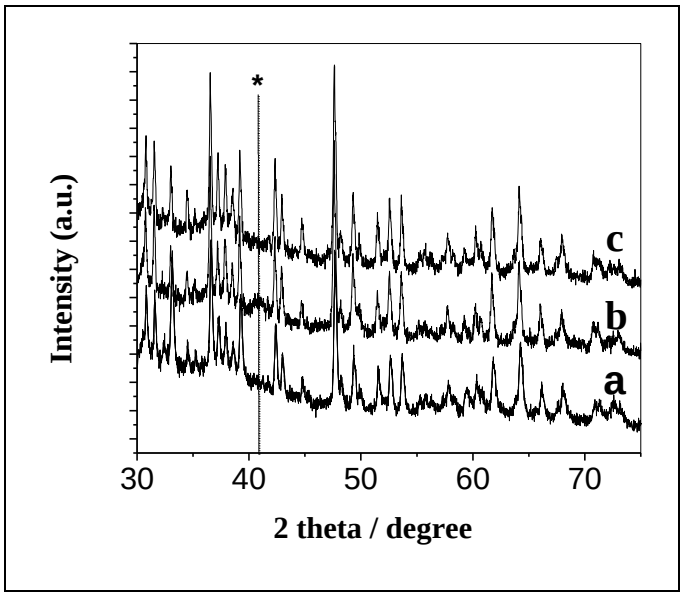

Figure 1: XRD patterns of the catalysts calcinated at different temperature (a) Rh/5A–200; (b) Rh/5A–400; (c) Rh/5A–500

XPS:

Chemical states of surface atoms in the catalysts after activity tests were investigated by XPS. Rh (3d) X-ray photoelectron spectra obtained from the Rh/5A samples calcined at different temperature (Figure 2), showed that for samples calcined at temperature of 400 ^{0}C and lower, the signal was comprised of a marked doublet which we ascribe to the presence of cationic rhodium (Figure 2a). It was possible that the shift in binding energy was associated with a relatively sharp bimodal particle size distribution but the bright field microscopy we had carried out does not reveal this to be the case. It was possible that very small rhodium particles such as those observed in the dried sample might be present in all sample and we were conducting more detailed microscopy study. The Rh (4f) spectrum observed after calcination at 600 ^{0}C shown a significant increase in line-width, consistent with the diffusion of Rh from the pores of the catalyst, and agglomeration to form metallic rhodium particles.

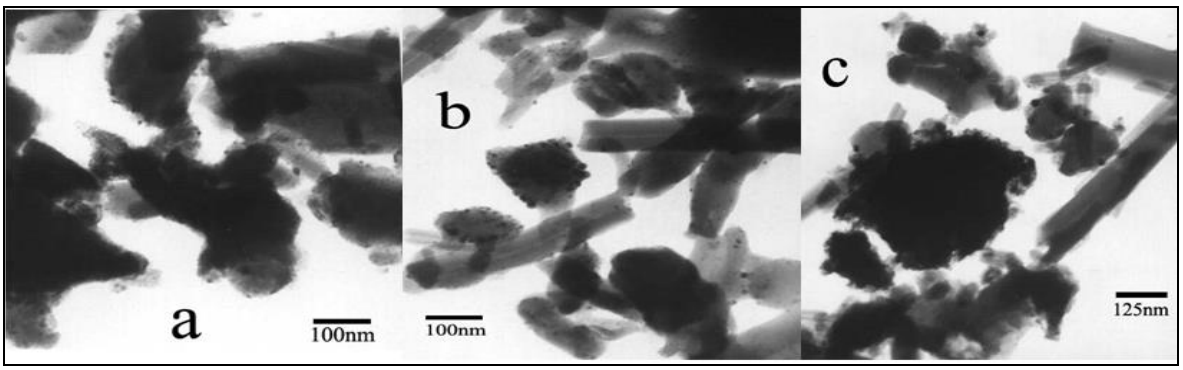

Figure 2: XPS data of Rh/5A catalysts calcined at different temperatures: (a) Rh/5A–200; (b) Rh/5A–300; (c) Rh/5A–400; (d) Rh/5A–500

TEM:

To observe directly the metallic particles in the three calcined samples, (a) 200 ^{0}C, (b) 400 ^{0}C, and (c) 600 ^{0}C. We performed TEM measurement after PROX activity tests on the catalysts and the result is shown in Figure 2. It shown TEM images of Rh particles were seen as dark contrasts on the surface of 5A-zeolite particles. At Rh/5A-200 (Figure 3a), most of metallic particles were observed dispersing with almost same size and a few large particles were

also observed. The loading state of the small particles may be obtained under the restricted condition against the diffusion of ion-exchanged Rh species and the growth of metallic particles due to the low temperature pretreatment and the limiting space of 5A zeolite cages. Image sizes of some metallic particles look larger than the pore diameter, but the sizes were not always necessary less than the pore diameter because of such reasons as electron scattering effect by the pore walls or overlapping of the particle images. Owing to the uniform particle dispersion and nearly the same sizes between the metallic particle diameter and the lattice spacing, it is presumed that these monodispersed particles were formed in 5A zeolite pores. Such small particles were not detectable by XRD, agreed with the results were shown in Figure 1a. At Rh/5A–400 (Figure 3b), large metallic particles with different sizes (5 nm in diameter) can be observed. Because the pore diameter of 5A zeolite is 0.5 nm, the large metallic particles should be supported on the outer surfaces. This suggests that the large particles were formed after calcination by coagulation of small particles. Rh particles on the 500^{o}C sample were much larger and show a much broader size distribution. Mean diameter and size distribution apparently increased from 200 ^{o}C to 500 ^{o}C. No particles with diameter below 10 nm were seen after calcination at this temperature.

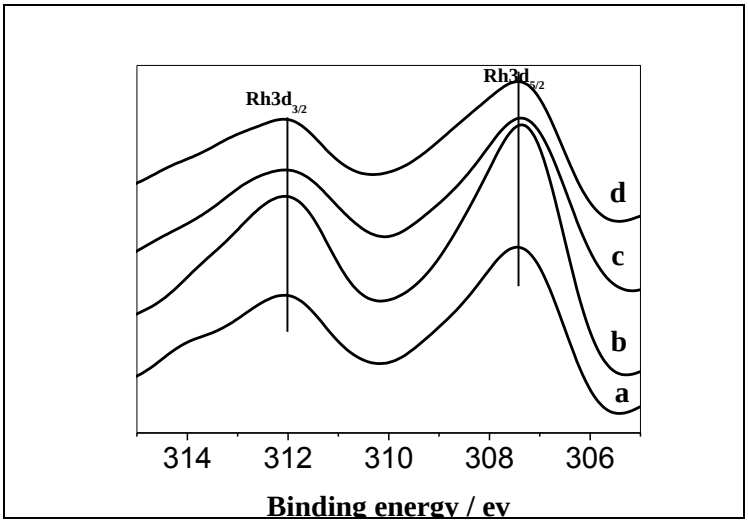

Figure 3: TEM pictures of the different catalysts: (a) Rh/5A-200; (b) Rh/5A–400; (c) Rh/5A–500

Activity measurements

Influence of Rh content on catalyse activity: Figure 4 showed the CO conversion over the Rh/5A catalysts with different Rh loading (0.4 –2 wt %). For all the Rh/5A samples, the activity for CO oxidation increased with the increase of the reaction temperature. It was interesting to note in Figure 4 that all catalysts exhibit a maximum in CO conversion with increasing temperature. The decline in CO conversion at elevated temperature was not due to the cool-down followed virtually the same path as run-up curves. The observed decrease in CO conversion with temperature appears to be related to the water-gas shift equilibrium limiting the CO conversion at high temperature, leading to consumption of the limited supply of O_2 in the feed by the H_2 in preference to the CO. At low temperatures, the CO conversion for 1.2 wt %/5A closely follows those for others, reaching 30 % at 70 ^{0}C. However, the CO conversion exhibited much weaker temperature dependence, diverging sharply from the conversion profiles for other loading Rh catalysts. Over the temperature range of interest in PROX operation (70–180 ^{0}C), the CO oxidation activity in the presence of excess H_2 decreases in the order: 1.2 wt % > 0.8 wt % > 2 wt % >1.6 wt % >0.4 wt %. This results indicated that increasing the Rh loading could promote the catalytic activities of the Rh/5A catalysts to some extent, but it was not always so. Among all these catalysts, the 1.2 wt % Rh/5A catalyst showed the highest catalytic activity and obtained complete CO conversion at 110 ^{0}C and at same time the selectivity of CO was 70 %, as shown in Figure 5. The similar results were reported by R. M. Friedman and J. Freeman, who pointed out that beyond a critical quantity, any additional copper loading was in the form of bulk crystalline oxide. Liu and Flytzani-stephanopoulos [18] suggested that the activity of catalyst derived primarily from the combination of finely dispersed copper-support systems, and bulk copper oxide had negligible contributions. Therefore, when the Rh loading was more than the monolayer dispersion threshold, the number of the effective active phase species was reduced with the increase of crystalline Rh resulting in a suppression of catalytic activity.

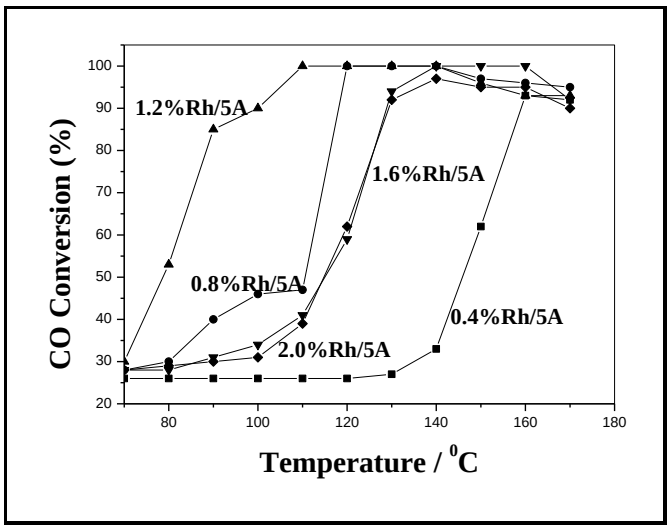

Figure 4: Relation between reaction temperature and CO conversion for catalysts with different Rh-loading. (The total flow rate of the feed gas was 75 ml min^{-1}. The feed gas consisted of 70 % of H_2, 2 % of CO and 1.4% of O_2 in N_2 balance.)

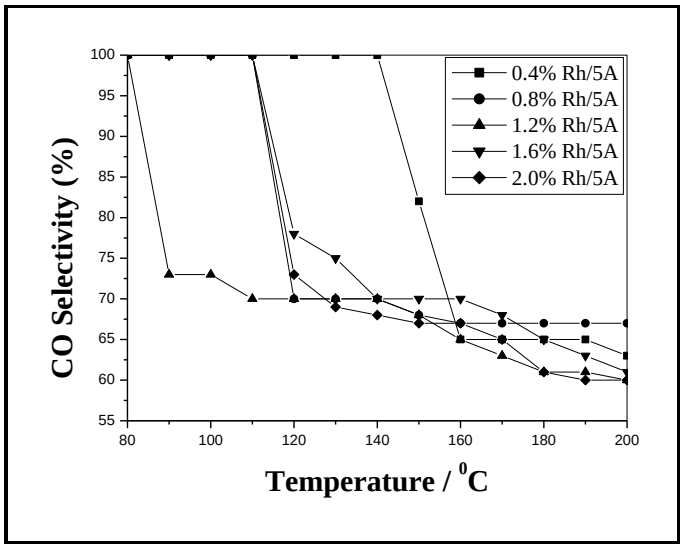

Figure 5: Relation between reaction temperature and CO selectivity for catalysts with different Rh-loading. (The total flow rate of the feed gas was 75 ml• min^{-1}. The feed gas consisted of 70% of H_2, 2% of CO and 1.4% of O_2 in N_2 balance.)

Ilaria Rosso [19] reported that the Pd and Ru-supported catalysts did not reach a complete CO-conversion, whereas the Pt-catalysts showed the highest CO-conversion and selectivity (The feed stream flow rate (100N·cm^3 min^{-1}) contained 37 vol.% H_2, 18 vol.% CO_2, 0.5 vol.% CO, 5 vol.% H_2O, 1 vol.% O_2, 39.5 vol.% He.). In particular, the 1% Pt/3A catalyst kept the complete CO-conversion in a wide temperature range, showing the highest selectivity for the CO oxidation with minimal involvement in side reactions, such as H_2 oxidation and RWGS reaction.

Influence of calcination temperature on catalyst activity: Figure 6 was given the CO oxidation activities on 1.2 wt % Rh/5A catalysts calcined at different temperature. It was found that the increase in calcination temperature of the catalysts resulted in a fluctuation of the CO oxidation activities. This results indicated that increasing the calcination temperature could promote the catalytic activities of the Rh/5A catalysts to some extent, but it was not always so. The activities of the catalysts increased by increasing the calcination temperature from 100 to 400 ^{0}C. When the reaction temperature increased from 80 to 110 ^{0}C, the conversion of CO increased from 20 to 30% on the

catalyst Rh/5A–100, and it could not reach 100% even at 180 ^{0}C. On the catalyst Rh/5A–400, however, the conversion of CO increased from 30 to 75 %, and CO converted completely at 120 ^{0}C. When we increased the calcination temperature of the catalyst further to 500 ^{0}C, the CO oxidation activities decreased considerably, no complete CO conversation was detected in the reaction temperature range of 60–180 ^{0}C. According to the XRD results, as the calcination temperature raised from 400 to 500 ^{0}C, the crystal size of Rh increased considerably. This suggested that the decrease of catalytic activity was caused by the increase of Rh crystal size.

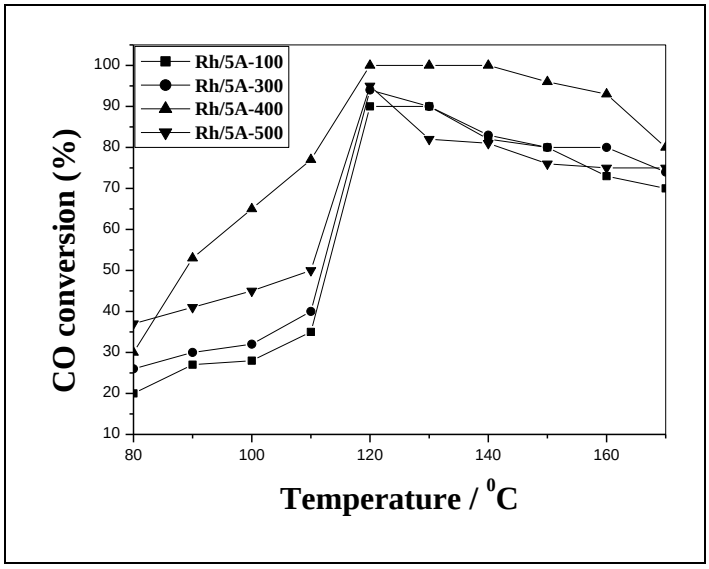

Figure 6: Relation between reaction temperature and CO conversion for catalysts calcinated at different temperature. (The total flow rate of the feed gas was 75 ml• min^{-1}. The feed gas consisted of 70 % of H_2, 2% of CO and 1.4% of O_2 in N_2 balance.)

From the XPS result we could know, as the calcinations temperature rose from 400 to 500 ^{0}C, the metal oxide disappeared and turned into metallic Rh. Metal and metal oxide surfaces are the most common surfaces on which reactions occur in heterogeneous catalysis. Thus, to understand the reactivity of these surfaces and the differences between them is of paramount importance. Although a new mechanism for CO oxidation has been identified by both experimental and theoretical works, there are still two fundamental issues remaining to be tackled: (I) Is it generally true that the activity of metal oxide is higher than that of the corresponding metal for CO oxidation? (ii) If the answer is yes, what is the origin of the activity increase from metals to metal oxides? Gong and co-workers [20] studied that the barrier on each metal oxide is significantly lower than that on the corresponding metal surface. These results indicate that in general the metal oxides are indeed more reactive than their corresponding metals for CO oxidation.

Study of thermal stability: To demonstrate the thermal stability of the catalyst involved in the reaction and the variation of different Rh species in the catalyst occurred during the catalytic reaction, cycle activity tests of the CO oxidation have been investigated over 1.2 wt % Rh/5A catalysts calcined at 400 ◦C. It can be seen from Figure 7 that the conversion of CO increased with increasing temperature. During the first run circle, when the temperature increased from 80 to 110 ◦C, the conversion of CO increased from 55 to 100%. While during the second run circle, the CO conversion decreased slightly, the CO converted 95% at 110 ^{o}C.

During the third run circle, the CO conversion decreased remarkably, it was only 75% even at 110 ^{o}C. It could be also found from that prolonging the reaction time results in lower CO conversion at a certain reaction temperature (such as 80-110 ^{o}C). Hence, the reaction appears to occur mainly on two types of catalytic centers, RhO_x and Rh, RhO_x is more active than metallic Rh. Therefore, in long term reaction by CO and H_2 results in low activity and hysteresis phenomena in catalytic cycles of CO oxidation.

When the temperature of total conversion of CO is reached, complete conversion of CO can be maintained in a long period with descending temperature. This is, perhaps, related to the thermal release of CO oxidation on reaction center, although the thermal detector shows descending environmental temperature.

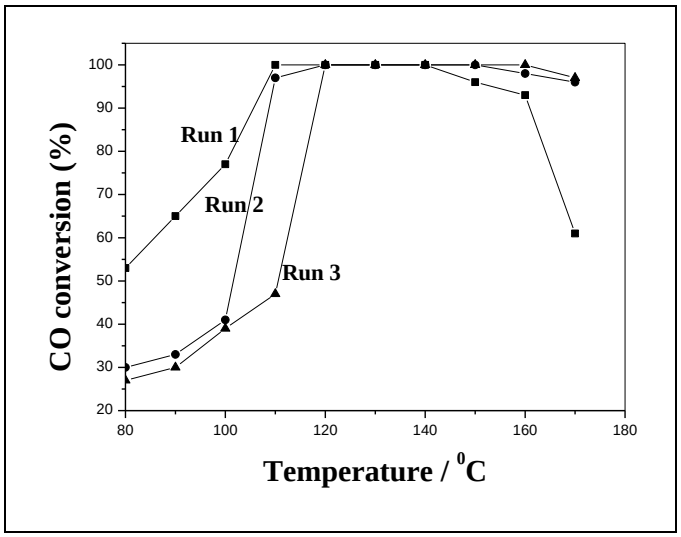

Figure 7: Study of thermal stability of the catalyst 1.2 % Rh/5A–400. (The total flow rate of the feed gas was 75 ml • min−1. The feed gas consisted of 70 % of H2, 2 % of CO and 1.4 % of O2 in N2 balance.)

Effect of moisture on stability: We have checked PROX activities on various catalysts in the gas mixture containing only CO, O_2 and H_2, so far. However, actual reformed gases contain both H_2O. Accordingly, we must test effects of H_2O on the PROX reaction at 1.2 wt % Rh/5A, which is crucial for the practical use. Based on the above results, a stability test of 1.2 wt % Rh/5A–400 in 2 % CO, 1.4 % O_2, 10 % H_2O, 70 % H_2 and N_2 balance was performed at 120 ^{0}C. Figure 8 depicts the variation of the catalytic activity of the catalyst for CO oxidation as a function of reaction time. Conversions of CO and O_2 reach to 100% even in the simulated gas containing H_2O. After 18 h, conversion was kept at 100% and the selectivity was also kept at 70%. The deactivation rate for 1.2 wt % Rh/5A catalyst was very low, and changed very slightly during the period of reaction time until the reaction was stopped (20 h). Although the longer-term durability test is essential for the practical application, at least we believe that the observed stability demonstrates the high potential of the catalyst application to the practical PROX reactor.

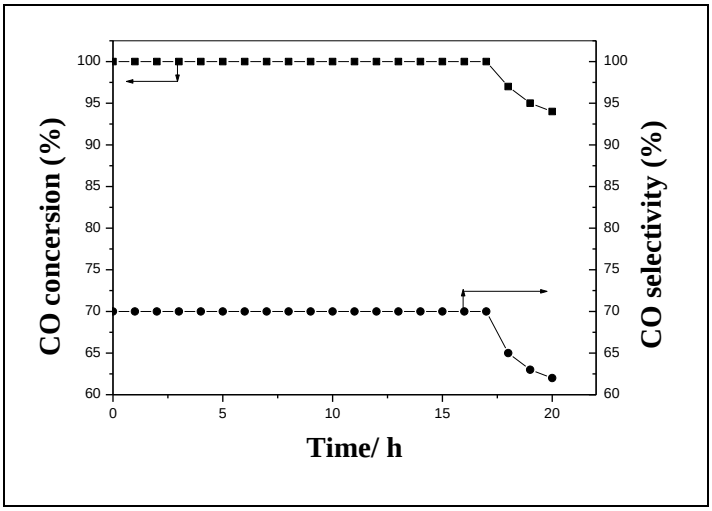

Figure 8: Influence of moisture on the activity of catalyst 1.2% Rh/ 5A–400. (The feed gas consisted of 70% of H_2, 2% of CO and 1.4% of O_2, 10% of H_2O and N_2 balance.)

CONCLUSIONS

The Rh/5A catalyst was proved to be an active and stable catalyst for CO selective oxidation. The 5A zeolite acted as the support and the Rh acted as the active component. The catalytic activity of the catalysts depended on some elements as follows:

(1) The Rh loading. The activity of Rh/5A catalysts with 1.2-wt % Rh loading was prior to the other catalysts. This might be due to the fact that 1.2-wt % Rh loading was near the monolayer dispersion threshold of Rh on 5A zeolite.

(2) Calcination temperature of the Rh/5A catalysts. The increase in CO oxidation activity of the Rh/5A catalysts with increasing calcination temperature from 200 to 400 ^{o}C could be attributed to the fact that the Rh was fully distribution outside of 5A zeolite and exist some cationic Rh, however, the decrease in catalytic activities with increasing calcination temperature from 400 to 500 ^{o}C could be attributed to the increase of the Rh crystalline size in the calcination process.

ACKNOWLDGEMENT

The work was supported by the Shandong Natural Science Foundation of China (ZR2014BL014), a Project of Shandong Province Higher Educational Science and Technology Program (J14LC54), a Project of Binzhou City science and technology development project (2014ZC0212) and Binzhou University (BZXYFB20140806 and 2010Y06.) research Funds.

REFERENCES

[1] R Fiorenza; C Crisafulli; GG Condorelli, et al. *Catalysis Letters*, **2015**, 145(9):1691-1702.
[2]N Sasirekha; P Sangeetha; YW Chen. *J Physical Chemistry C*, **2014**, 118(28):15226-15233.
[3] EDO Jardim; S Rico-Francés; Z Abdelouahab-Reddam, et al. *Applied Catalysis A General*, **2015**, 502:129-137.
[4] L Chen; Y Bao; Y Sun, et al. *Catalysis Science & Technology*, **2015**, 6(4):491-513.
[5] KW Jeon; DW Jeong; WJ Jang, et al. *Korean J Chemical Engg*, **2016**, 33(6):1-7.
[6] N Bion; F Epron; M Moreno, et al. *Topics in Catalysis*, **2008**, 51(1-4):76-88.
[7] H Guan; L Jian; L Lin, et al. *Applied Catalysis B Environmental*, **2015**, 184:299-308.
[8] A Baraldi; G Comelli; D Vr, et al. *Applied Surface Science*, **1996**, 99(1):1-8.
[10] MK Sun; K Qadir; B Seo, et al. *Catal Lett*, **2013**, 143(11):1153-1161.
[11] S Kim; K Qadir; S Jin et al. *Catal. Today*, **2012**, 185(1):131-137.
[12] S Ito; H Tanaka; Y Minemura; et.al. *Applied Catalysis A: General*, **2004**, 273(1), 295-302.
[13] SSC Chuang; CD Tan. *Catalysis Today*, **1997**, 35(4): 369-377.
[14] A Luengnaruemitchai; M Nimsuk; P Naknam et al. *Int J Hydrogen Energy*, **2008**, 33(1): 206-213.
[15] J Xu; XC Xu; L Ouyang et al. *[J]. J Catalysis*, **2012**, 287(3):114-123.
[16] I Rosso; C Galletti; S Fiorot, et al. *[J]. Catheterization & Cardiovascular Interventions*, **1999**, 46(4): 509-510.
[17] I Rosso; C Galletti; G Saracco, et al. *[J]. Applied Catalysis B: Environmental*, **2004**, 48(3):195-203.
[18] W Deng; C Carpenter; N Yi, et al. *[J]. Topics in Catalysis*, **2007**, 44(1-2):199-208.
[19] I Rosso; C Galletti; G Saracco et al. *[J]. Applied Catalysis B Environmental.*, **2004**, 48(3):195-203.
[20] XQ Gong; ZP Liu; R Raval. *J. Am. Chem. Soc.*, **2004**,126, 8-9.